ACCOUNTS
of chemical research

Kinetic Products in Coordination Networks: Ab Initio X-ray Powder Diffraction Analysis

JAVIER MARTÍ-RUJAS[†] AND MASAKI KAWANO[*,‡]

[†]*Italian Institute of Technology, Centre for Nano Science and Technology (CNST—IIT@PoliMi), Via Pascoli 70/3, 20133 Milan, Italy, and* [‡]*The Division of Advanced Materials Science, Pohang University of Science and Technology (POSTECH), San 31 Hyojadong, Pohang 790-784, Korea*

RECEIVED ON JULY 18, 2012

CONSPECTUS

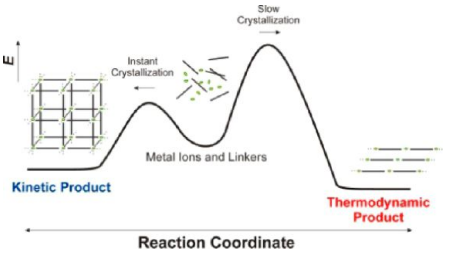

Porous coordination networks are materials that maintain their crystal structure as molecular "guests" enter and exit their pores. They are of great research interest with applications in areas such as catalysis, gas adsorption, proton conductivity, and drug release. As with zeolite preparation, the kinetic states in coordination network preparation play a crucial role in determining the final products. Controlling the kinetic state during self-assembly of coordination networks is a fundamental aspect of developing further functionalization of this class of materials. However, unlike for zeolites, there are few structural studies reporting the kinetic products made during self-assembly of coordination networks. Synthetic routes that produce the necessary selectivity are complex.

The structural knowledge obtained from X-ray crystallography has been crucial for developing rational strategies for design of organic—inorganic hybrid networks. However, despite the explosive progress in the solid-state study of coordination networks during the last 15 years, researchers still do not understand many chemical reaction processes because of the difficulties in growing single crystals suitable for X-ray diffraction: Fast precipitation can lead to kinetic (metastable) products, but in microcrystalline form, unsuitable for single crystal X-ray analysis. X-ray powder diffraction (XRPD) routinely is used to check phase purity, crystallinity, and to monitor the stability of frameworks upon guest removal/inclusion under various conditions, but rarely is used for structure elucidation. Recent advances in structure determination of microcrystalline solids from ab initio XRPD have allowed three-dimensional structure determination when single crystals are not available. Thus, ab initio XRPD structure determination is becoming a powerful method for structure determination of microcrystalline solids, including porous coordination networks. Because of the great interest across scientific disciplines in coordination networks, especially porous coordination networks, the ability to determine crystal structures when the crystals are not suitable for single crystal X-ray analysis is of paramount importance.

In this Account, we report the potential of kinetic control to synthesize new coordination networks and we describe ab initio XRPD structure determination to characterize these networks' crystal structures. We describe our recent work on selective instant synthesis to yield kinetically controlled porous coordination networks. We demonstrate that instant synthesis can selectively produce metastable networks that are not possible to synthesize by conventional solution chemistry. Using kinetic products, we provide mechanistic insights into thermally induced (573—723 K) (i.e., annealing method) structural transformations in porous coordination networks as well as examples of guest exchange/inclusion reactions. Finally, we describe a memory effect that allows the transfer of structural information from kinetic precursor structures to thermally stable structures through amorphous intermediate phases.

We believe that ab initio XRPD structure determination will soon be used to investigate chemical processes that lead intrinsically to microcrystalline solids, which up to now have not been fully understood due to the unavailability of single crystals. For example, only recently have researchers used single-crystal X-ray diffraction to elucidate crystal-to-crystal chemical reactions taking place in the crystalline scaffold of coordination networks. The potential of ab initio X-ray powder diffraction analysis goes beyond single-crystal-to-single-crystal processes, potentially allowing members of this field to study intriguing in situ reactions, such as reactions within pores.

Published on the Web 12/19/2012 www.pubs.acs.org/accounts
10.1021/ar300212v

Introduction

Porous coordination networks have emerged as one of the key materials in the 21st century because of the high designability and the simple preparation methods. Thanks to the hybrid nature of their building blocks (metal ions and organic ligands),[1−6] porous coordination networks have been used in areas such as gas adsorption,[7−10] catalysis,[11−13] proton conductivity,[14−16] and drug release.[17,18] Porous coordination networks are usually synthesized in "one-pot" reactions with slow crystallization methods like layer diffusion or solvothermal synthesis. The self-assembled building blocks tend to produce thermally stable crystals suitable for single crystal X-ray diffraction. Unlike zeolites, coordination networks often display flexibility as well as rigidity,[19,20] which have enhanced dramatically their potential applications. Metastable products often as intermediates are, on the other hand, produced as a result of kinetic reactions and are of fundamental importance in many processes involving organic,[21] inorganic,[22] and biological systems.[23] Thus, the ability to control the synthesis and the structural characterization of metastable products is important to create new materials.

Single crystal X-ray analysis is the most reliable technique to determine the structure of crystalline porous coordination networks. However, one of the limitations of single crystal X-ray analysis is that rather often single crystals of suitable size and crystallinity cannot be obtained. Unfortunately, fast crystallization methods tend to form kinetic microcrystals and therefore their structural characterization has to be carried out using ab initio X-ray powder diffraction. Structure determination of microcrystalline coordination networks is considerably more challenging than single crystal analysis. Porous coordination networks tend to have large unit cells and often low symmetry that contribute to severe peak overlap, hampering unit cell determination, the most crucial step in structure determination. However, despite its complexity, crystal structures that were not accessible from single crystal X-ray diffraction have been studied using X-ray powder diffraction analysis.[24−30]

This Account describes our work in which we have been exploiting the potential of kinetic control and ab initio XRPD to study chemical processes in porous coordination networks. We describe the selective instant synthesis of kinetically controlled porous coordination networks, and structural transformations as well as high temperature solid-state reactions by using microcrystalline solids and guest exchange/inclusion reactions.

Coordination Networks and X-ray Powder Diffraction

There are several algorithms that allow ab initio structure determination, but it is out of the scope of this Account to go into detailed description.[31] However, we want to mention some approaches that various groups have adopted to solve crystal structures of microcrystalline porous coordination networks that are different from the one we have used. Mellot-Draznieks et al. and Férey et al. in 2005 reported a chromium teraphthalate-based porous coordination network (MIL-101) with a giant unit cell ($V = 702\,000$ Å^3) and extra large pores (Figure 1a).[24,25] Structure solution was carried out using computer simulation by employing the global optimization AASBU (Automated Assembly of Secondary Building Units) method which explores combinations of inorganic clusters with organic ligands that form 3D periodic lattices. From the frameworks obtained, a XRPD pattern is simulated and compared with the experimental one until a good match is obtained. Then the structure was refined by the Rietveld method and guest molecules located from Fourier difference maps. Kitagawa et al. reported the adsorption of C_2H_2 in a microporous coordination network using synchrotron X-ray data and MEM (Maximum Entropy Minimization) analysis (Figure 1b).[27] The MEM analysis allowed computing the guest electron density map, revealing the precise host−guest interaction. Guest C_2H_2 molecules are oriented in the channel toward the two noncoordinated oxygen atoms on the pore wall by hydrogen bonding (2.2 Å), allowing a dense packing of C_2H_2. Yaghi et al. recently reported a series of conductive isoreticular coordination networks with tunable pore size using the newly developed charge-flipping algorithm (Figure 1c).[28,29] The good crystallinity of the networks allowed indexing of the unit cell and space group assignment. The structures were corroborated by successful Rietveld refinement.

Ab Initio X-ray Powder Diffraction in Porous Coordination Networks: Instant Synthesis Method

Kinetic control in the synthesis of porous coordination networks is potentially very important, as it allows the formation of structures that usually are not "isolated" by slow crystallization. Kinetic metastable products tend to transform toward more stable structures. In general, thermodynamic

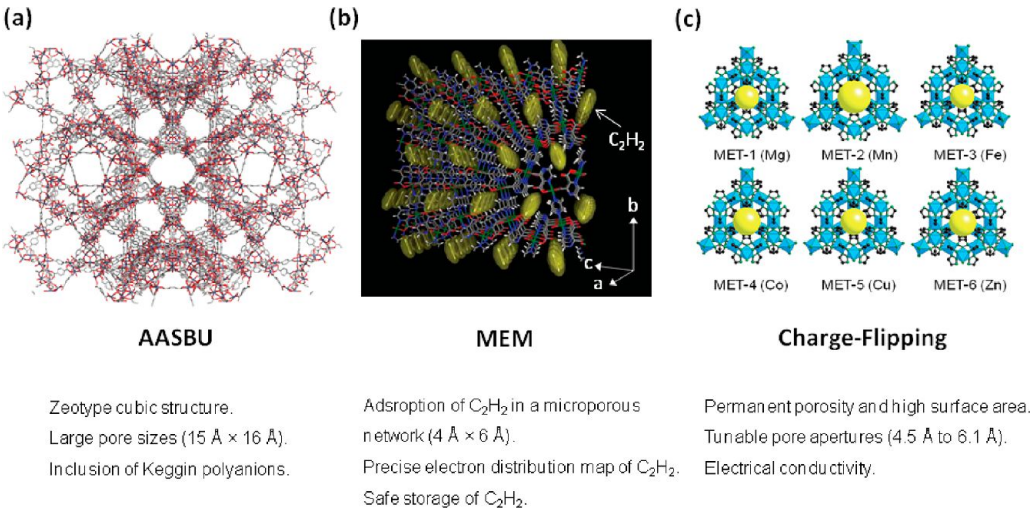

FIGURE 1. Examples of crystal structures of coordination networks solved by ab initio X-ray powder diffraction.

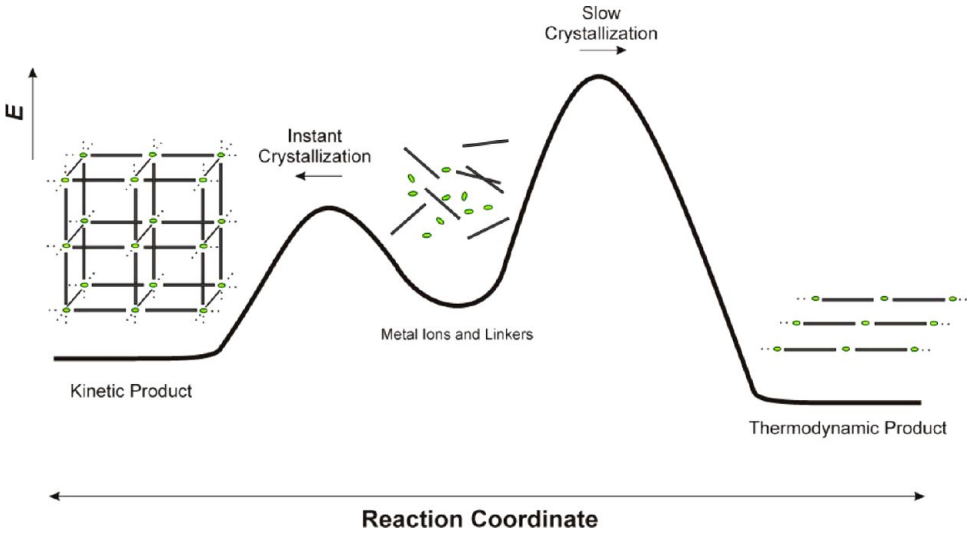

FIGURE 2. Reaction pathway in instant synthesis and slow crystallization methods.

products are formed by slow complexation and can be characterized by single crystal X-ray analysis, while kinetic products yield microcrystalline powders and rarely can be solved by the single crystal method (Figure 2). Obtaining a pure phase by slow complexation is not straightforward, as often mixed products precipitate. Therefore, we developed the *instant synthesis* (i.e., a 30 s time frame crystallization period) method which is a simple process enabling the selective formation of homogeneous products in which a metal solution is added instantaneously to a vigorously stirred ligand saturated solution. As a result, a microcrystalline product (kinetic) is obtained immediately whose structure is different from that obtained by slower crystallization techniques such as layering diffusion or solvothermal methods (thermodynamic) (Figure 2). In some cases where the pores are large and filled with solvent, due to high flexibility of porous coordination networks, grinding of single crystals usually tends to amorphization or poor crystallinity. Thus, the instant synthesis can be regarded as selective crystallization method.

Fast addition of a methanol solution of ZnX_2 (where X = I, Br, Cl) into a vigorously stirred nitrobenzene/methanol solution of 2,4,6-tris(4-pyridyl)triazine (TPT) resulted in crystals with similar shape and average particle size of ca. 10 μm within 30 s. Elemental analyses indicated the composition $[(ZnX_2)_3(TPT)_2]\cdot 5(\text{solvent})$ (solvent = $C_6H_5NO_2\cdot H_2O$) **1**–**3** (Figure 3).

Crystal structures of **1** and **2** were successfully solved by ab initio synchrotron XRPD despite having large unit cell volumes (over 15 000 Å^3).[32] Synchrotron XRPD pattern was indexed to give a monoclinic unit cell with good figures of

merit followed by profile refinement using the Pawley method. Structure solution was performed by the simulated annealing method (i.e., global optimization method) implemented in the DASH computer program[33] followed by Rietveld refinement using RIETAN-FP program.[34] Rietveld refinement (Figure 4) confirmed the good agreement between the experimental and simulated XRPD patterns.

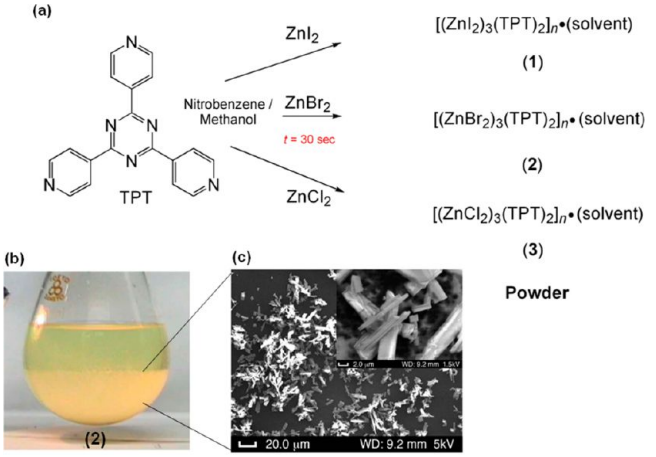

FIGURE 3. (a) Instant synthesis of isostructural porous coordination networks **1**–**3**. (b) View of the microcrystalline powder of **2** (at bottom of round-bottom flask) obtained after the instant synthesis method and (c) SEM image of the powder.

Networks **1**–**3** are described as a 10,3-*b* type network,[35] show interpenetration, and have large channels containing nitrobenzene. The channels are interconnected in two directions to yield a 2D channel network with a free volume amounting to ca. 50% of the unit cell volume (Figure 4). Due to the large solvent content in the crystal structure, the channels are like small reactor vessels, a concept that has been recently referred as crystalline molecular flask.[36]

To prove that the instant synthesis method selectively produces only one product, a slow crystallization method was set up by layered solution with the same stoichiometric ratio of starting reagents for **2**. After 1 week (vide infra) (Figure 5b), needle crystals $[(ZnBr_2)_3(TPT)_2]\cdot 6(C_6H_5NO_2)$ (**4**) were collected (75% yield). The thermodynamic product (*Fdd*2) belongs also to the 10,3-*b* type network without interpenetration and forms large 1D pores (ca. 25 Å) including nitrobenzene (Figure 5c). Network **4** is extremely flexible. In a guest exchange reaction, the original nitrobenzene molecules in **4** were replaced by TTF and cyclohexane in a single-crystal-to-single-crystal (SCSC) process. The framework suffered a considerable deformation following a unit

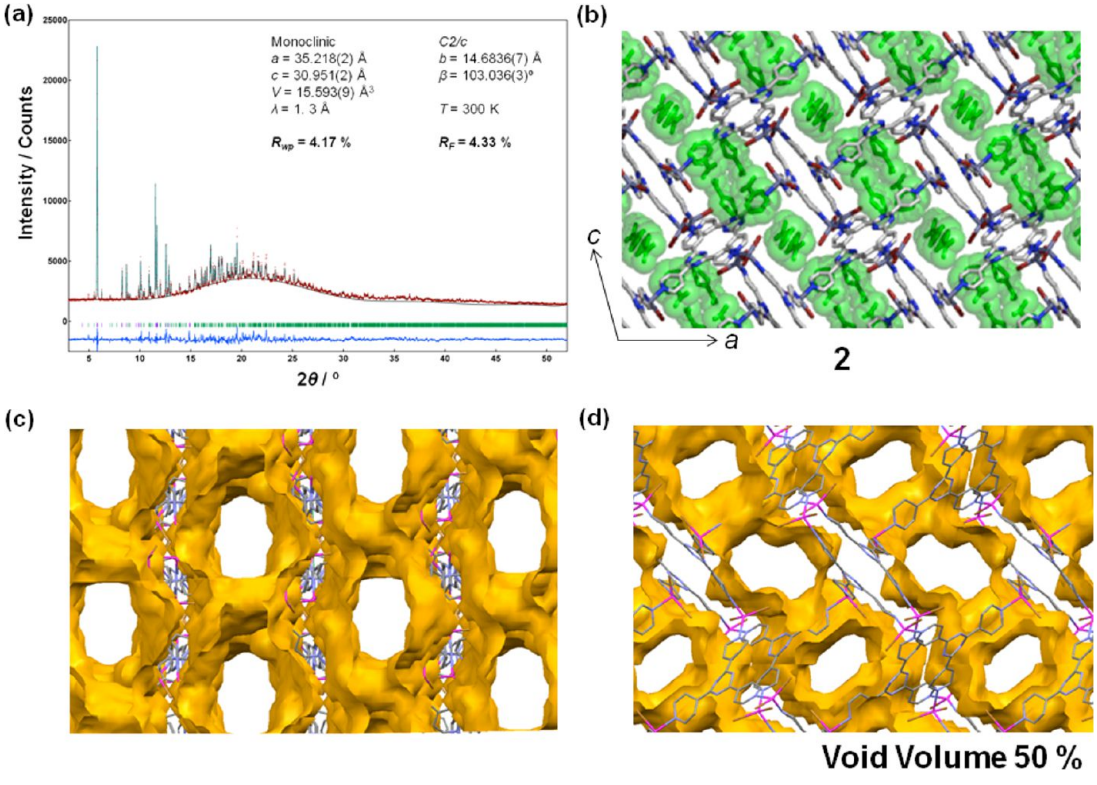

FIGURE 4. (a) Rietveld refinement of **2**. Experimental (red), calculated (pale blue), and difference (dark blue) X-ray powder diffraction profile. (b) Rietveld crystal structures of **2** viewed along the *b*-axis. Nitrobenzene is shown in green. Void volume (1.4 Å probe radius) of the framework showing the dimensions and the shape of the accessible voids: view (c) along the 101 direction and (d) along the *b*-axis.

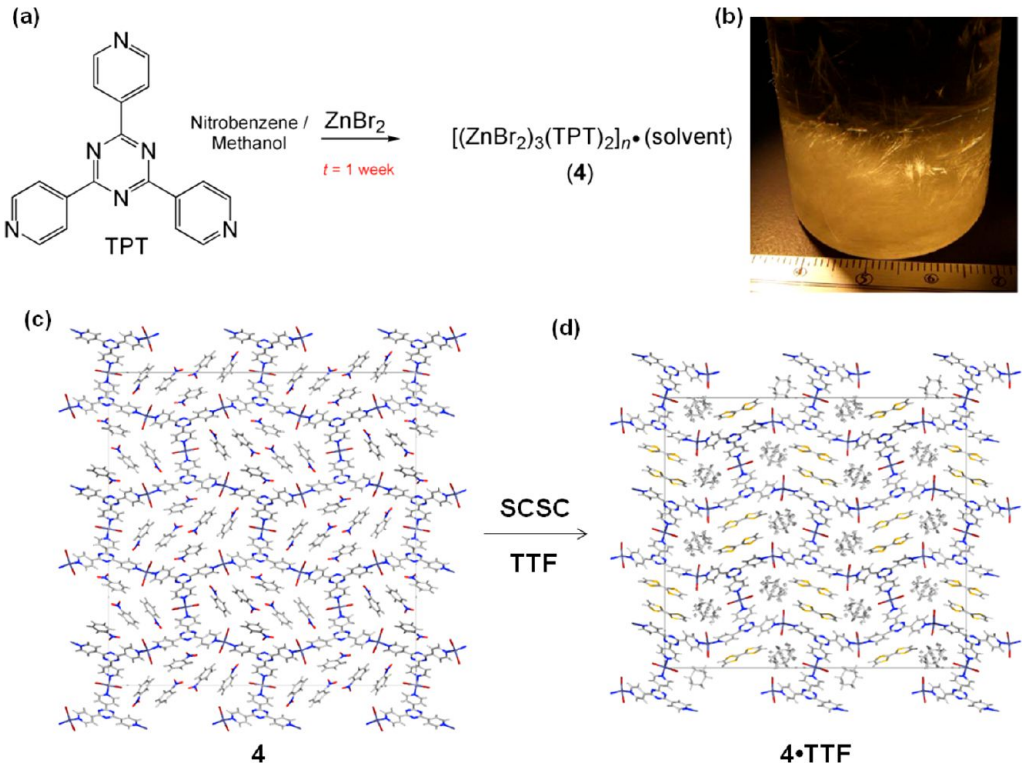

FIGURE 5. (a) Synthesis of thermodynamic crystals **4** obtained by layering diffusion of $ZnBr_2$ (methanol) onto a TPT (nitrobenzene) solution. (b) Needlelike single crystals of **4** grown in a vessel over 1 week. (c) Crystal structure of **4** (d) deformation in the framework in **4** caused by the inclusion of TTF (**4**·**TTF**) molecules following a SCSC reaction.

cell volume reduction of ca. 1759 $Å^3$ with a shortening of the *a*-axis from 49.547 to 43.973 Å while keeping crystallinity (Figure 5d). The same type of crystals are obtained when $ZnCl_2$ (**5**) is used instead of $ZnBr_2$.

Using the instant synthesis method, larger and more complex porous coordination networks could be obtained by adding a large templating molecule (triphenylene).[37] A new microcrystalline powder was prepared by fast addition of a methanol solution of $ZnBr_2$ into a vigorously stirred nitrobenzene/methanol solution of TPT and triphenylene (Tr). Within 30 s, a yellow powder precipitated and then isolated in 60% yield by filtration (Figure 6). Elemental analysis indicated that the compound $[(ZnBr_2)_3(TPT)_2(Tr)]\cdot$(solvents) (**6**) was obtained.

The agreement between experimental and calculated diffraction patterns in the Rietveld refinement plot indicates correctness of the structure despite the large unit cell volume (ca. 17 000 $Å^3$). In **6**, triphenylene molecules are intercalated between TPT ligands templating the formation of the network while nitrobenzene fills the pores. The structure has two different pores and infinite alternation of TPT-Tr molecules along *b*-axis (A and B, in Figure 7). Pore A is roughly cylindrical and is mainly surrounded by the hydrogen atoms of stacked triphenylene. Pore B is trigonal prismatic surrounded by three walls: two of them are π-faces of ligand TPT, and the third corresponds to the edges of TPT and triphenylene.

Also in this case, if a layered solution with the same stoichiometries of reagents is prepared, large single crystals (Figure 6) of a nonporous structure are obtained. Triphenylene molecules are stacked between TPT ligands in a TPT−TPT−Tr pattern forming 1D chains as a thermodynamic product (**7**) (Figure 8). Moreover, we observed that if the kinetic network (**6**) prepared by the instant synthesis is left in the solution at 295 K within a week, large needle crystals of **7** are obtained.

This type of open frameworks usually cannot be grinded due to their softness as often they become amorphous. Clearly, the advantage of the instant synthesis method is that it produces homogeneous crystals and there is little need to homogenize the particle size by grinding to avoid preferential orientation in the powder X-ray analysis.

The instant synthesis method allows the selective formation of kinetic products rather than thermodynamic structures, showing the potential of this method for the preparation of new compounds that are difficult or impossible by conventional crystallization. New porous coordination chemistry can be exploited by using the instant synthesis method.

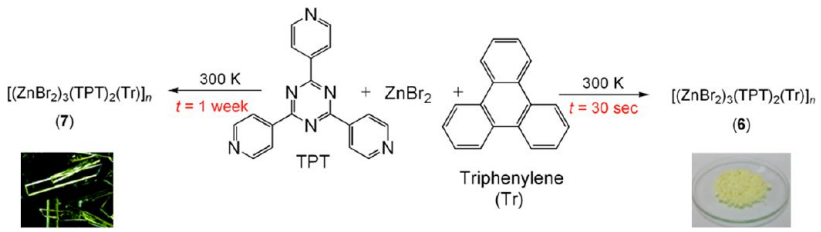

FIGURE 6. Synthesis of kinetically controlled porous network (**6**) and thermodynamically controlled nonporous coordination network (**7**).

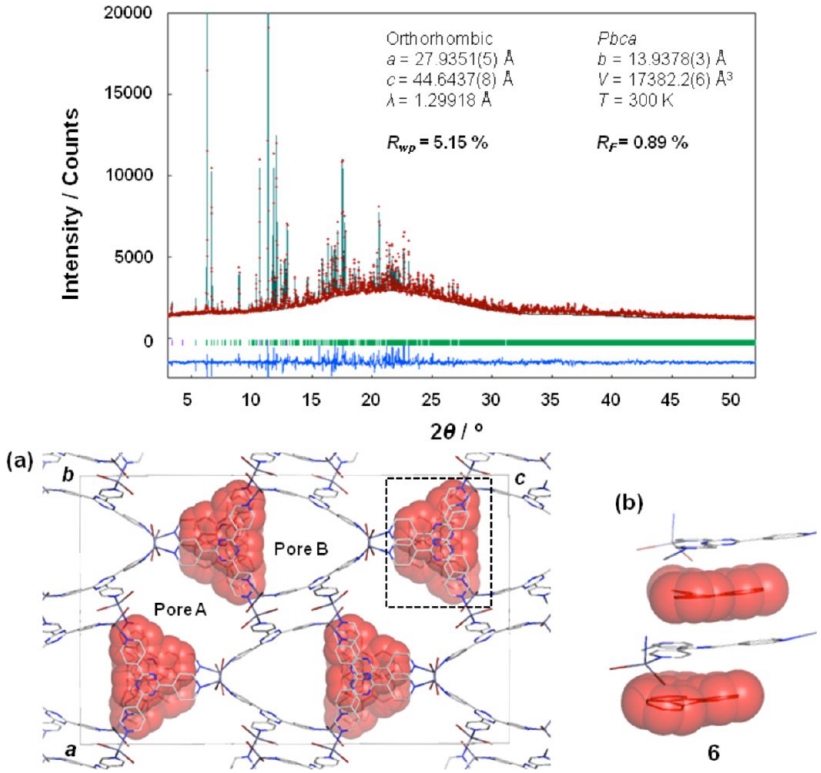

FIGURE 7. Top: Rietveld refinement of **6**. Experimental (red), calculated (pale blue), and difference (dark blue) X-ray powder diffraction profile. (a) Rietveld crystal structure of network complex **6** viewed along the *b*-axis. Nitrobenzene molecules in the pores are omitted for clarity. (b) Detailed view of the infinite aromatic stacking of ligand TPT and triphenylene molecules (red).

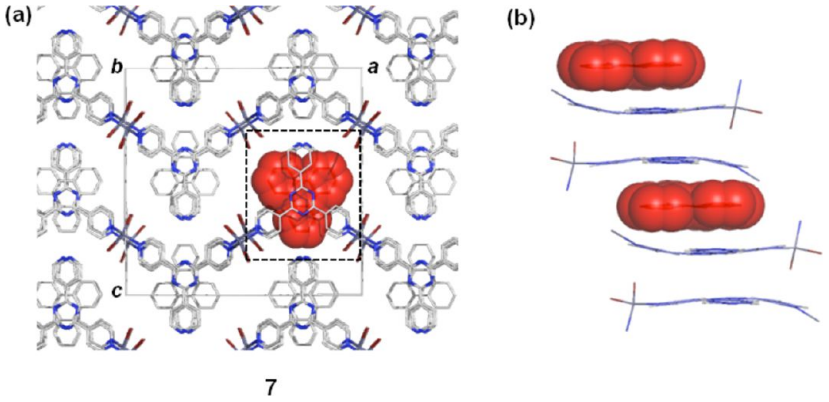

FIGURE 8. (a) Single crystal X-ray diffraction structure of thermodynamic **7** showing the 1D chains running along the *a*-axis. Nitrobenzene molecules are omitted for clarity. (b) View of the infinite stacking of TPT and triphenylene (red) along the *c*-axis.

High Temperature Solid-State Reactions Involving Intermediate Amorphous Phases

Kinetic metastable structures tend to transform toward more stable structures. Therefore, we can use the prearrangement in the metastable structures to form new structures that are not possible to form in solution-state reactions.

Among the most studied solid-state transformations in porous coordination networks are guest exchange and photoinduced reactions as such reactions can be followed by SCSC processes.[38,39] Due to the formation of the product within the lattice of the reactant, solid-state reactions often destroy the lattice of the reactant. Paradoxically, the SCSC is a sort of limitation in the solid-state chemistry of porous coordination networks because many solid-state processes finish in polycrystalline phase. Thus, single-crystal-to-polycrystalline reactions in porous coordination networks were not completely explored because single crystal X-ray diffraction was not feasible. We are interested in the understanding of solid-state reactions that proceed at high temperatures, typically involving temperatures in which organic ligands decompose or sublime. Through high temperature solid-state reactions, severe structural transformations involving cleavage and formation of coordination bonds and intermediate amorphous phases do occur, and we have recently demonstrated that using the state-of-the-art ab initio X-ray powder diffraction studies.

Kinetically controlled metastable compounds **1**−**3** were synthesized with the instant synthesis method and monitored above 573 K. It is known that **1** can shrink and swell upon guest removal by mild heating (343 K),[40] but what happens to **1** above 343 K was unknown.

Microcrystals of **1** were heated from 300 to 673 K and monitored by in situ synchrotron XRPD.[41] The diffraction experiments showed two phase transitions involving an intermediate amorphous phase (Figure 9a).

Such crystalline-to-amorphous-to-crystalline (CAC) phase transitions are not common in porous coordination networks. The new phase obtained after the amorphous phase is different from that of **1** and thermally stable up to 673 K. Supporting our X-ray analysis, thermogravimetric analysis-differential scanning calorimetry (TG-DSC) experiments revealed that nitrobenzene molecules are progressively released (300 to 473 K) and that a new and homogeneous crystalline phase is formed at 573 K, as an exothermic peak is observed in the DSC agreeing with XRPD data (Figure 9b). Elemental analysis suggests the chemical formula $[(ZnI_2)_3(TPT)_2]_n$ (**8**) allowing crystal structure determination by synchrotron ab initio XRPD[41] followed by Rietveld refinement (Figure 10).

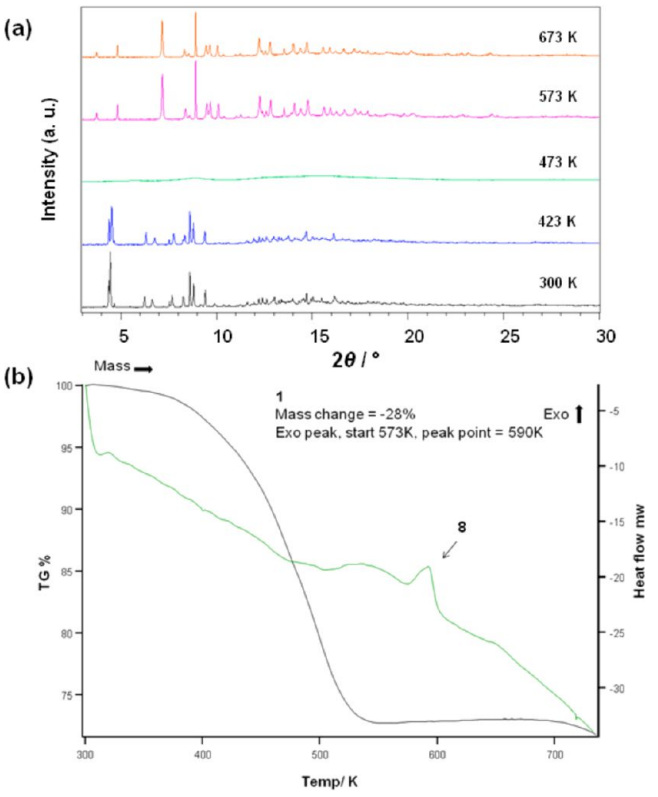

FIGURE 9. (a) In situ synchrotron XRPD patterns of **1** at various temperatures. An intermediate phase is observed at 473 K indicating that significant structural transformation occurs during the solid-state process. Recrystallization and formation of a new crystalline solid occurs at 543 K and is stable up to 673 K. (b) TG-DSC analysis shows the release of nitrobenzene followed by crystallization (**8**) as observed in the DSC analysis as an exothermic peak.

In **8**, two molecules of TPT are connected through two ZnI_2 forming a "saddle-type" structure extending along the *b*-axis as 1D chains (Figure 10b and c). Adjacent chains held together by intermolecular $\pi-\pi$ interactions between stacked pyridyl and triazine rings along the *c*-axis gives rise to the formation of noninterpenetrated 1D channels with pore windows of ca. 6.2 Å × 8.5 Å. Network **8** is stable under vacuum at low as well as high temperatures (95−673 K) and can undergo liquid−solid and gas−solid inclusion reactions.[42] One year later, we reported a microcrystalline isostructural network applying a solid−liquid interface reaction and determined its structure by ab initio XRPD.[43]

The structural transformation in this CAC reaction involves the unlocking of the initial interpenetrated 10,3-*b* type network and formation of a different 1D chain. First, guest removal and shrinking of the networks occurs, followed by unlocking of interpenetrated networks by cleavage of coordination bonds, and crystallization by bond formation to yield the new porous coordination network.

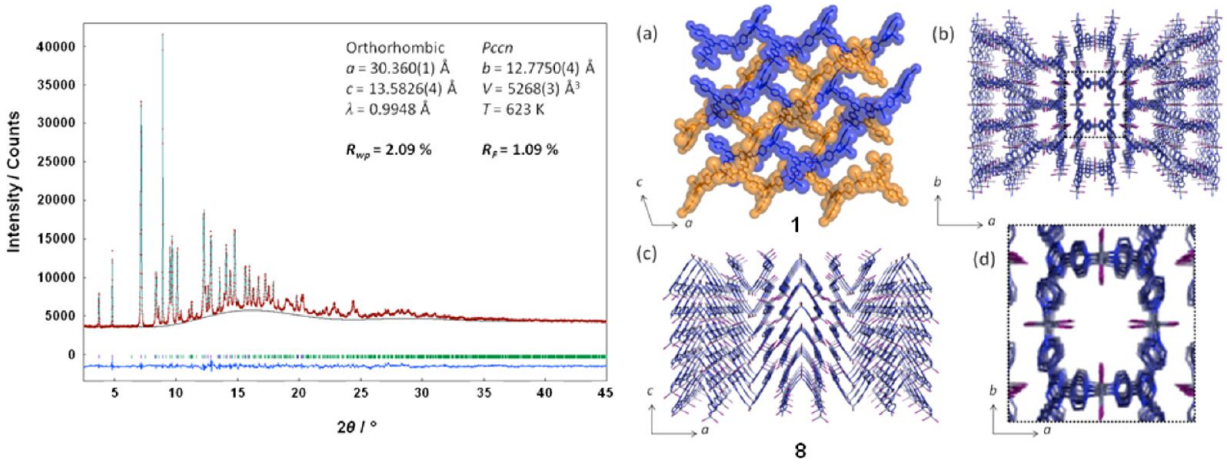

FIGURE 10. Left: Experimental (red), calculated (pale-blue), and difference (dark-blue) XRPD profiles from the final Rietveld refinement of **8**. (a) Crystal structure of **1** showing the interpenetration of two networks (blue and orange). (b) Noninterpenetrated structure of **8** viewed along the pore direction. (c) "Saddle-type" structure in **8**. (d) Detailed view of the pore.

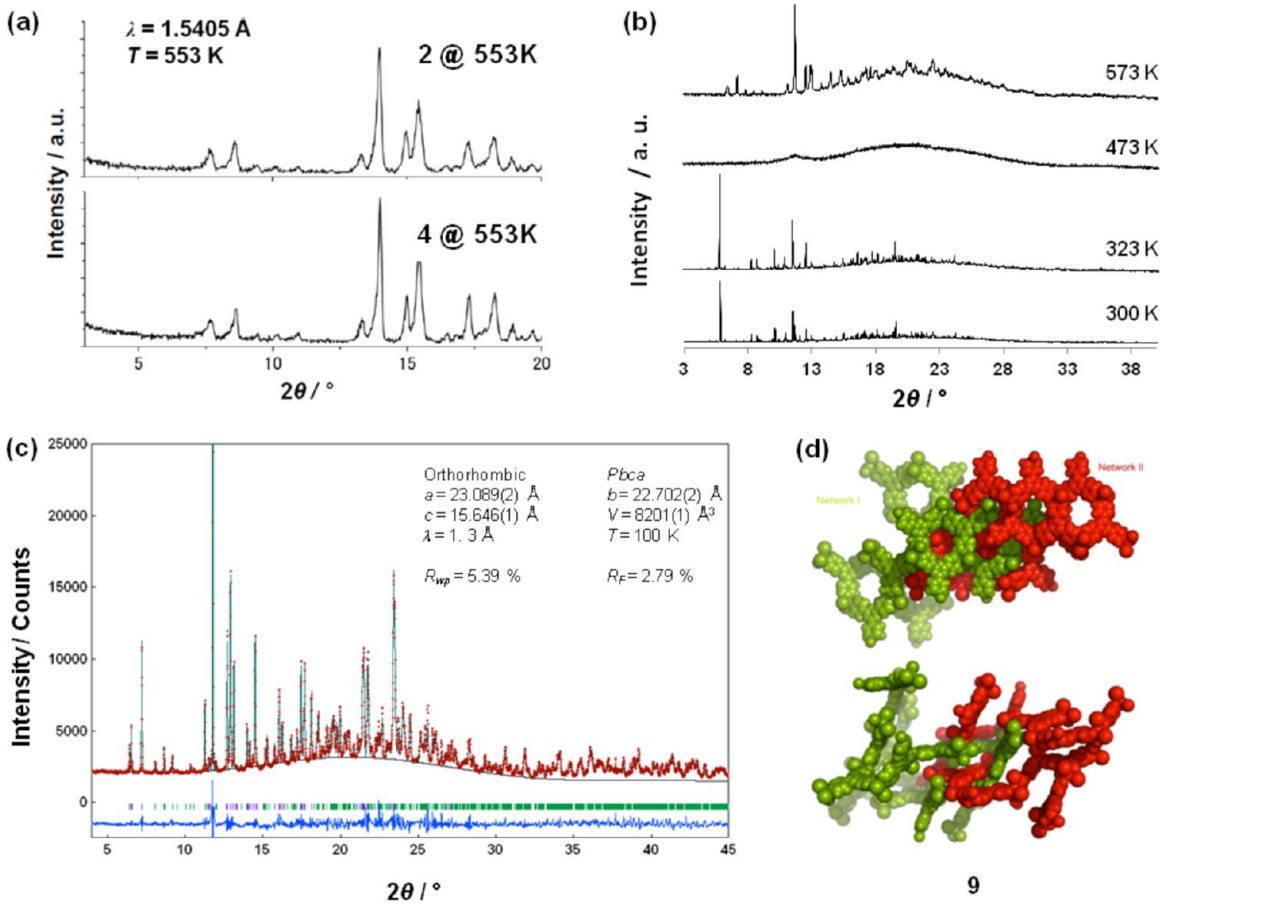

FIGURE 11. (a) XRPD patterns obtained after heating at 553 K interpenetrated **2** and noninterpenetrated **4** networks. (b) In situ synchrotron XRPD patterns of **2** at different temperatures showing a CAC transformation. A new crystalline phase appears at 573 K. (c) Rietveld refinement of **9** obtained at high temperature. (d) Crystal structure of **9** with the two interpenetrating circuits (green and red) formed after the CAC transformation viewed along the *c*-axis (top) and side view (bottom).

The annealing method for the synthesis of highly crystalline materials has been widely used in ceramics and zeolites[44] but not in porous coordination networks. We believe that high temperature synthesis in coordination

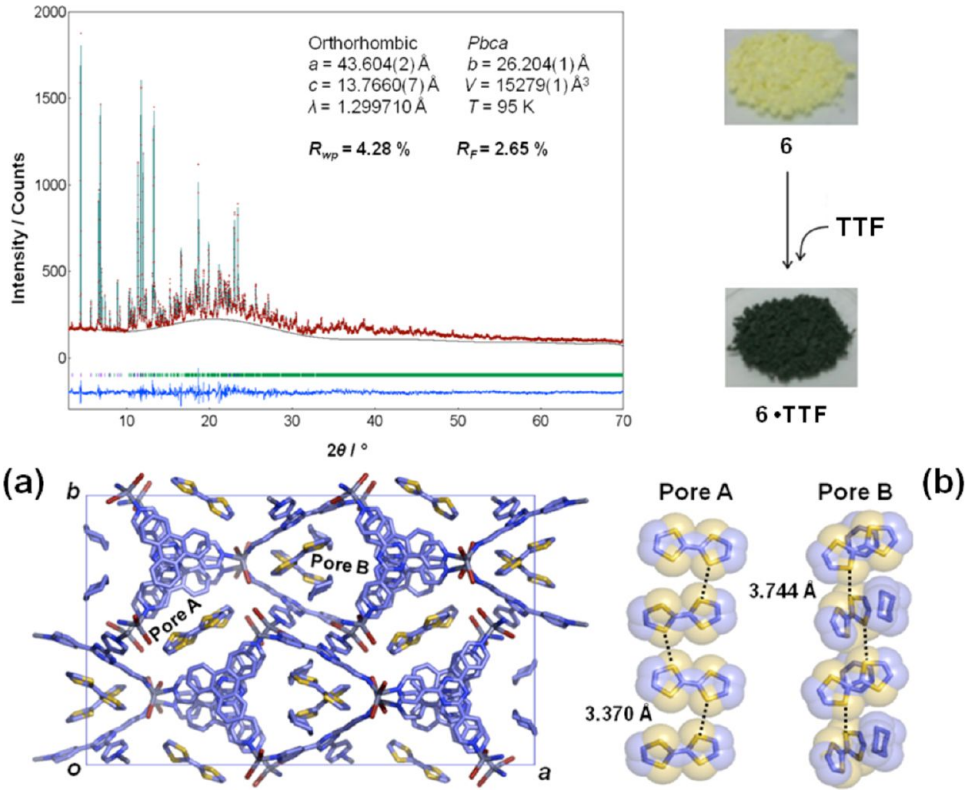

FIGURE 12. Top left: Experimental (red), calculated (pale-blue), and difference (dark-blue) XRPD profiles from the final Rietveld refinement of (**6**·**TTF**). Top right: Color change in **6** (yellow) observed in the guest inclusion of TTF and formation of **6**·**TTF** (dark green). (a) Crystal structure of (**6**·**TTF**) determined directly from ab initio synchrotron XRPD data. Pores A and B contain TTF molecules and cyclohexane is included only in pore B. (b) Detailed view of pores A and B.

networks can produce new solids with interesting properties, as already shown in the synthesis of a fluorinated coordination network able to selectively separate hydrocarbons without taking up water.[45]

Exploiting ab Initio XRPD Analysis in the Solid-State Chemistry of Porous Coordination Networks

Mechanistic Aspects in Annealed Solid-State Reactions. Intrigued by the results observed in **1**, we investigated compounds **2** and **3** that differ only in the zinc halide. Although **1**−**3** are isostructural, upon heating from 300 to 723 K, they result in three different products despite following the same type of CAC phase transitions. We demonstrated that kinetic (**2**) and thermodynamic (**4**) networks after CAC result in the same XRPD pattern upon heating (Figure 11a and b).

Crystal structure determination from ab initio XRPD shows that the new phase (**9**) is a double interpenetrated network, proving again (as observed in **1**) that to go from noninterpenetrated (**4**) to interpenetrated (**9**) bond-breaking and bond forming occurs during the CAC phase transformation (Figure 11c and d). Surprisingly, further heating to 723 K and slow cooling of **2** produced high quality single crystals with a new bromide-bridged network.[42] Here, the high temperature produced some calcination and most likely partial melt of **2** that upon slow cooling allowed the formation of high quality single crystals. Similarly, the chloride version **3** also through a CAC formed a new phase but not stable enough so that it transformed to a new chloride-bridged network at 723 K.[42]

Amorphous phases are intriguing because unlike crystalline phases we cannot know their three-dimensional arrangement by X-ray diffraction. Looking carefully at the diffraction pattern of the amorphous phase, the two broad "peaks" at ca. $2\theta = 13°$ and $2\theta = 23°$ (Figure 11b) suggests that long-range order still exists in the solid and hence allowing the building of new structures. We demonstrated by TG-DSC and XRPD that mixing ZnX_2 (where X = I or Br) and ligand TPT using the same stoichiometric amounts of starting materials as in instant synthesis, followed by mixing, grinding and heating, did not form **8** nor **9**. Thus, to a certain degree some structural memory from the metastable phases is retained in the amorphous phase and transferred to the more stable structure.

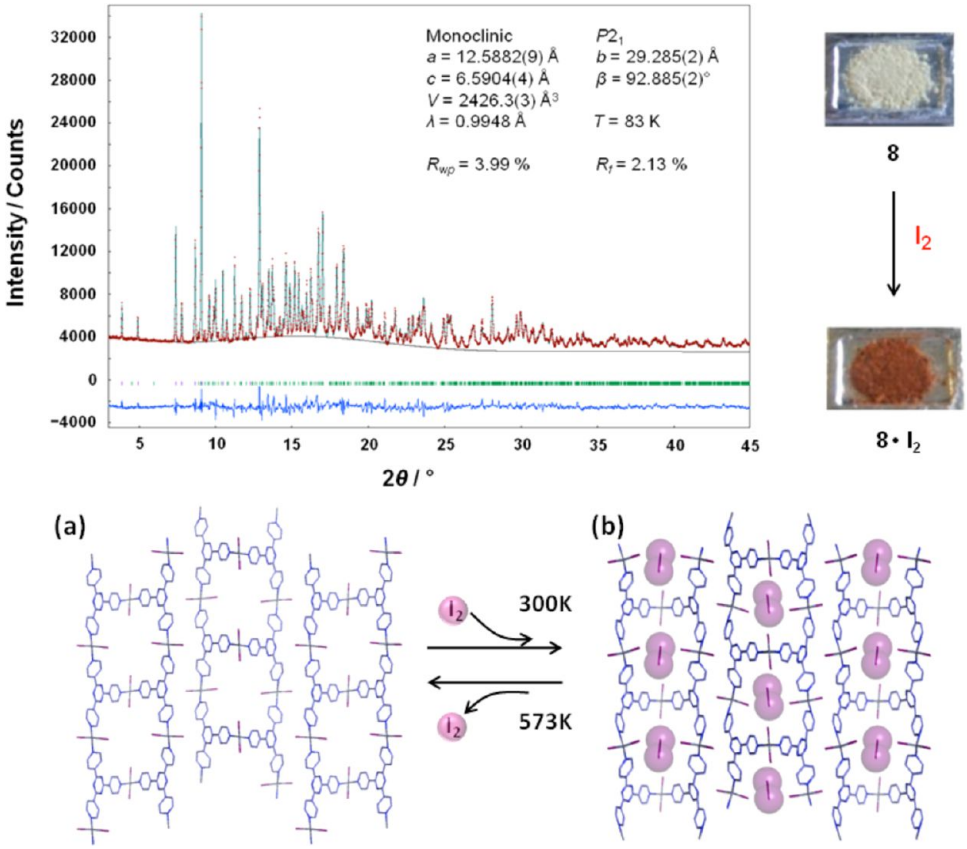

FIGURE 13. Top left: Experimental (red), calculated (pale-blue), and difference (dark-blue) XRPD profiles from the final Rietveld refinement of **8·I$_2$** (top). Top right: Color change of **1** upon exposure to vapors of I_2. Reversible guest inclusion/removal of I_2 in **1** (bottom).

Pore-Shape Directed Guest Alignment via Guest Exchange Reactions. In supramolecular chemistry, the ability to control the position of noncovalently bound molecules (guests) located in cavities such as channels or cages is important. Large channels can accommodate molecules that tend to be disordered, but in particular cases the network pore can induce guest alignment resulting in unique arrangements.

The precise alignment of TTF molecules within a porous network has been achieved by using a kinetically synthesized microcrystalline biporous coordination network (**6**). The selective formation of **6** was possible using the instant synthesis method as layering diffusion yields nonporous network **7**.[37] Using pore confinement effect, we succeeded in aligning TTF molecules, by carrying a guest exchange reaction after immersing microcrystalline **6** in a TTF-cyclohexane solution. The polycrystalline-to-polycrystalline guest exchange reaction was clearly observed by the color change from yellow to dark green while maintaining good crystallinity. The color change indicates charge-transfer interactions between host and TTF. To fully determine the crystal structure, ab initio XRPD analysis was carried out followed by Rietveld refinement. The agreement between the calculated and the experimental XRPD patterns in the final Rietveld refinement indicates that the structure is correct (Figure 12). In the crystal structure, $[(ZnBr_2)_3(TPT)_2(Tr)]_n \cdot (TTF)_2 \cdot (C_6H_{12})$, (**6·TTF**) TTF molecules are included in pores A and B and cyclohexane molecules are only in pore B (Figure 12), in agreement with elemental analysis.

We demonstrated that by changing the metal halide two isostructural porous coordination networks have different guest inclusion ability. Under the same conditions for the guest exchange reaction, TTF molecules are included only in one pore (A) if the ZnI_2 is used, but using $ZnBr_2$ allows the inclusion of TTF molecules in both pores. Size difference in halides as well as different strength-flexibility in Zn-halide coordination bonds can explain the different TTF inclusion behavior. The S···S distances among stacked TTFs in pore A of (**6·TTF**) are shorter (ca. 3.370 Å) than those in pore B (3.744 Å). In both pores, the TTF molecules are not stacked through $\pi-\pi$ interactions but rather via S···S contacts probably due to the pore confinement effect (Figure 12b). Such a short contact among TTFs may allow conductivity along the pores. However, due to small crystal size (<10 μm),

single crystal conductivity measurement was unsuccessful and instead measurement using pellets after gently grinding the network showed no conductivity.

Reversible Guest Inclusion via Solid–Liquid and Gas–Solid Reactions. Like carbon-based materials and zeolites, porous coordination networks also can be used for many applications in catalysis, conductivity, sensors and separation, mainly due to their tunable pore size, shape and chemical environment. Among the various applications, separation is one of the most used in porous coordination networks. In this regard, recently a porous coordination network has shown that can adsorb CO_2 using a combination of suitable pore size and functionalization even at low pressures.[46]

As shown in Figure 10, **8** has 1D channels suitable to accommodate guest molecules. We demonstrated the guest inclusion ability by immersing **8** in nitrobenzene for 30 min. TG-DSC confirmed that one nitrobenzene molecule was included in the network and it was corroborated by elemental analysis and XRPD. Crystal structure determination carried out by ab initio synchrotron XRPD showed the inclusion of nitrobenzene (**8**·$\mathbf{G_1}$) and swelling of the framework. To determine the nitrobenzene position precisely, the crystal structure analysis was carried out at 95 K.[41] The inclusion/removal of nitrobenzene is reversible, as heating up to 573 K the original structure with empty channels was formed.

We also investigated the gas-phase inclusion of I_2 in **8**.[42] After exposing **8** to vapors of I_2 at 300 K overnight, the yellow solid turned brown (Figure 13) and the XRPD pattern showed a peak shift and change in the relative intensities suggesting the inclusion of I_2. After the inclusion of I_2, the crystallinity was good and the XRPD pattern was indexed successfully. Ab initio XRPD structure solution confirmed the **8**·$\mathbf{I_2}$ formation.

The I_2 molecules are located between iodide atoms of ZnI_2 units at the center of the pore with intermolecular distance along the *c*-axis of 6.59 Å. The I_2 and the iodide from the ZnI_2 form a 1D array through halogen bonding interactions.[47] We note that the framework shapes itself in the presence of different guest molecules. When bulky nitrobenzene is included in **8**, the framework swells, whereas it shrinks upon I_2 adsorption even when the two crystal structures have been solved at low temperatures (95 and 83 K, respectively). Such detailed structural analysis of organic–inorganic materials is trivial in single crystal X-ray analysis but not in ab initio XRPD analysis.

Concluding Remarks

Nature inspires us to learn from chemical processes observed in biological systems. Nature uses kinetic processes to keep biological systems alive, whereas thermodynamic state usually means conformations that hardly change, which means the end of life activity. In the solid state, kinetic solids are often produced in fast processes leading to microcrystalline solids that are difficult to be studied by single crystal X-ray diffraction. In fact, many interesting materials are obtained as microcrystals where the limitation of single crystal X-ray diffraction analysis often stops the possibility of further understanding of new chemical reactions. Here, we reported examples of chemical processes that produce microcrystalline kinetic materials, including synthesis from solution and suspensions. We have used those metastable kinetic products (i.e., as precursors) to study mechanistic aspects in solid-state reactions at elevated temperatures. The high temperature solid-state reactions occur via intermediate amorphous phases that retain structural information (memory effect) from the kinetic structure which is passed to more stable structures upon heating. In particular cases, the high temperature products can be porous, allowing guest inclusion/exchange reactions. Ab initio XRPD structure determination will be exploited soon to study microcrystalline products such as the ones described here, and others that lead intrinsically to powder solids. For instance, in situ XRPD studies in crystalline pores can provide relevant information in chemical reactions that often have been left aside because single crystals are not available. Kinetic products often can produce structures with pores larger than those obtained through thermodynamic processes, which can lead to functional materials upon inclusion of guests such as pollutant gas molecules or molecules with photophysical or conductive properties. In addition, kinetic assembly of open-shell species can produce metastable spin states by suppressing spin–spin repulsion which may show unique dynamic physical properties. We believe that kinetic study of solid state materials on the basis of structural chemistry will lead to development of a new class of materials.

This research was supported by WCU (World Class University) program (Project No. R31-2008-000-10059-0) and Basic Research (Project No. 2011-0009930) through the Korea Science and Engineering Foundation funded by the Ministry of Education, Science and Technology. We thank the Japan Society for the Promotion of Science (fellowship to J.M.-R.) for funding and our collaborators in our papers for their generous support. This work was approved by SPring-8 (Proposals 2008A1843 and 2008A1938). Single crystal and powder X-ray diffraction experiments were performed at the Pohang Accelerator Laboratory

(beamlines 6B1 and 8C2) supported by Pohang University of Science and Technology.

BIOGRAPHICAL INFORMATION

Javier Martí-Rujas received his Ph.D. in solid state chemistry at Cardiff University with Prof. Kenneth D. M. Harris in 2005. After two postdoctoral experiences at Georgetown University (2006) and Cardiff University (2007), he moved as JSPS fellow to The University of Tokyo. After 2 years in Japan, he joined as Senior Postdoctoral fellow the Center for Nano Science and Technology at the Italian Institute of Technology in Milan. In 2012, he was promoted to a Research Technologist. He works on host−guest chemistry of porous solids and organic supramolecular structures.

Masaki Kawano has been Professor at Pohang University of Science and Technology, Korea since 2009. He received his Ph.D. in Coordination Chemistry at Waseda University with Prof. Kazuko Matsumoto in 1993. He became Assistant Professor at the same school (1992−1994). He experienced Postdoctoral positions at the University of Wisconsin—Madison (1994−1997) and Tokyo Institute of Technology (1997−2003). Then he moved to the University of Tokyo as a Lecturer (2003−2004) where he was promoted to Associate Professor until 2009. His research interests include self-assembled materials and in/ex situ chemical crystallography.

FOOTNOTES

*To whom correspondence should be addressed. E-mail: mkawano@postech.ac.kr.
The authors declare no competing financial interest.

REFERENCES

1 Hoskins, B. F.; Robson, R. Infinite polymeric frameworks consisting of three dimensionally linked rod-like segments. *J. Am. Chem. Soc.* **1989**, *111*, 5962–5964.

2 Subramanian, S.; Zaworotko, M. J. Porous solids by design: $[Zn(4,4'\text{-bpy})_2(SiF_6)]_n \cdot xDMF$, a single framework octahedral coordination polymer with large square channels. *Angew. Chem., Int. Ed.* **1995**, *34*, 2127–2129.

3 Yaghi, O. M.; Li, H. Hydrothermal synthesis of a metal-organic framework containing large rectangular channels. *J. Am. Chem. Soc.* **1995**, *117*, 10401–10402.

4 Eddaoudi, M.; Moler, D. B.; Li, H.; Chen, B.; Reineke, T. M.; O'Keeffe, M.; Yaghi, O. M. Modular chemistry: secondary building units as a basis for the design of highly porous and robust metal-organic carboxylate frameworks. *Acc. Chem. Res.* **2001**, *34*, 319–330.

5 Kitagawa, S.; Kitaura, R.; Noro, S. Functional porous coordination polymers. *Angew. Chem., Int. Ed.* **2004**, *43*, 2334–2375.

6 Férey, G. Hybrid porous solids: past, present, future. *Chem. Soc. Rev.* **2008**, *37*, 191–214.

7 Kondo, M.; Yoshitomi, T.; Seki, K.; Matsuzaka, H.; Kitagawa, S. Three-dimensional framework with channeling cavities for small molecules: $\{[M_2(4,4'\text{-bpy})_3(NO_3)_4] \cdot xH_2O\}_n$ (M = Co, Ni, Zn). *Angew. Chem., Int. Ed. Engl.* **1997**, *36*, 1725–1727.

8 Zhao, X.; Xiao, B.; Fletcher, A. J.; Thomas, K. M.; Bradshaw, D.; Rosseinsky, M. J. Hysteretic adsorption and desorption of hydrogen by nanoporous metal-organic frameworks. *Science* **2004**, *306*, 1012–1015.

9 Takamizawa, S.; Nataka, E.; Akatsuka, T.; Miyake, R.; Kakizaki, Y.; Takeuchi, H.; Maruta, G.; Takeda, S. Crystal transformation and host molecular motions in CO_2 adsorption process of a metal benzoate pyrazine (M^{II} = Rh, Cu). *J. Am. Chem. Soc.* **2010**, *132*, 3783–3792.

10 Bloch, E. D.; Queen, W. L.; Krishna, R.; Zadrozny, J. M.; Brown, C. M.; Long, J. R. Hydrocarbon separations in a metal-organic framework with open Iron(II) coordination sites. *Science* **2012**, *335*, 1606–1610.

11 Fujita, M.; Kwon, Y. J.; Washizu, S.; Ogura, K. Preparation, clathration ability, and catalysis of a two-dimensional square network material composed of cadmium(II) and 4,4′-bipyridine. *J. Am. Chem. Soc.* **1994**, *116*, 1151–1152.

12 Seo, J.-S.; Whang, D.; Lee, H.; Jun, S. I.; Oh, J.; Jeon, Y. J.; Kim, K. A homochiral metal-organic porous material for enantioselective separation and catalysis. *Nature* **2000**, *404*, 982–986.

13 Farha, O. K.; Shultz, A. M.; Sarjeant, A. A.; Nguyen, S. T.; Hupp, J. T. Active-site-accessible, porphyrinic metal−organic framework materials. *J. Am. Chem. Soc.* **2011**, *133*, 5652–5655.

14 Hurd, J. A.; Vaidhyanathan, R.; Thangadurai, V.; Ratcliffe, C. I.; Moudrakovski, I. L.; Shimizu, G. K. H. Anhydrous proton conduction at 150 °C in a crystalline metal-organic framework. *Nat. Chem.* **2009**, *1*, 705–710.

15 Bureekaew, S.; Horike, S.; Higuchi, M.; Mizuno, M.; Kawamura, T.; Tanaka., D.; Yanai., N.; Kitagawa, S. One-dimensional imidazole aggregate in aluminium porous coordination polymers with high proton conductivity. *Nat. Mater.* **2009**, *8*, 831–836.

16 Shigematsu, A.; Yamada, T.; Kitagawa, H. Wide control of proton conductivity in porous coordination polymers. *J. Am. Chem. Soc.* **2011**, *133*, 2034–2036.

17 Della Rocca, J.; Liu, D.; Lin, W. Nanoscale metal-organic frameworks for biomedical imaging and drug delivery. *Acc. Chem. Res.* **2011**, *44*, 957–968.

18 Horcajada, P.; Gref, R.; Baati, T.; Allan, P. K.; Maurin, G.; Couvreur, P.; Férey, G.; Morris, R. E.; Serre, C. Metal−Organic Frameworks in Biomedicine. *Chem. Rev.* **2012**, *112*, 1232–1268.

19 Horike, S.; Shimomura, S.; Kitagawa, S. Soft porous crystals. *Nat. Chem.* **2009**, *1*, 695–704.

20 Horcajada, P.; Salles, F.; Wuttke, S.; Devic, T.; Heurtaux, D.; Maurin, G.; Vimont, A.; Daturi, M.; David, O.; Magnier, E.; Stock, N.; Filinchuk, Y.; Popov, D.; Riekel, C.; Férey, G.; Serre, C. How linker's modification controls swelling properties of highly flexible Iron (III) dicarboxylates MIL-88. *J. Am. Chem. Soc.* **2011**, *133*, 17839–17847.

21 Percec, V.; Hudson, S. D.; Peterca, M.; Leowanawat, P.; Aqad, E.; Graf, R.; Spiess, H. W.; Zeng, X.; Ungar, G.; Heiney, P. A. Self-repairing complex helical columns generated via kinetically controlled self-assembly of dendronized perylene bisimides. *J. Am. Chem. Soc.* **2011**, *133*, 18479–18494.

22 Zhu, M.; Lanni, E.; Garg, N.; Bier, M. E.; Jin, R. Kinetically controlled, high-yield synthesis of Au_{25} clusters. *J. Am. Chem. Soc.* **2008**, *130*, 1138–1139.

23 Hwang, W.; Zhang, S.; Kamm, R. D.; Karplus, M. Kinetic control of dimer structure formation in amyloid fibrillogenesis. *Proc. Natl. Acad. Sci. U.S.A.* **2004**, *101*, 12916–12921.

24 Mellot-Draznieks, C.; Newsam, J. M.; Gorman, A. M.; Freeman, C. M.; Férey, G. De novo prediction of inorganic structures developed through automated assembly of secondary building units (AASBU method). *Angew. Chem., Int. Ed.* **2000**, *39*, 2270–2275.

25 Férey, G.; Mellot-Draznieks, C.; Serre, C.; Millange, F.; Dutour, J.; Surblé, S.; Margiolaki, I. A chromium terephthalate-based solid with unusually large pore volumes and surface area. *Science* **2005**, *309*, 2040–2042.

26 Kondo, M.; Okubo, T.; Asami, A.; Noro, S.; Yoshitomi, T.; Kitagawa, S.; Ishii, T.; Matsuzaka, H.; Seki, K. Rational synthesis of stable channel-like cavities with methane gas adsorbtion properties: $[\{Cu_2(pzdc)_2(L)\}_n$ (pzdc = pyrazine-2,3-dicarboxylate; L = a pillar ligand). *Angew. Chem., Int. Ed.* **1999**, *38*, 140–143.

27 Matsuda, R.; Kitaura, R.; Kitagawa, S.; Kubota, Y.; Belosludov, R. V.; Kobayashi, T. C.; Sakamoto, H.; Chiba, T.; Takata, M.; Kawazoe, Y.; Mita, Y. Highly controlled acetylene accomodation in a metal-organic microporous material. *Nature* **2005**, *436*, 238–241.

28 Gándara, F.; Uribe-Romo, F. J.; Britt, D. K.; Furukawa, H.; Lei, L.; Cheng, R.; Duan, X.; O'Keeffe, M.; Yaghi, O. M. Porous, conductive metal-triazolates and their structural elucidation by the charge flipping method. *Chem.—Eur. J.* **2012**, *18*, 10595–10601.

29 Oszlányi, G.; Sütő, A. Ab initio structure solution by charge flipping. *Acta Crystallogr., Sect. A* **2004**, *60*, 134–141.

30 Harris, K. D. M.; Cheung, E. Y. How to determine structures when single crystals cannot be grown: opportunities for structure determination of molecular materials using powder diffraction data. *Chem. Soc. Rev.* **2004**, *33*, 526–538.

31 David, W. I. F.; Shankland, D.; McCusker, L. B.; Baerlocher, C., Eds. *Structure Determination from Powder Diffraction Data*; IUCr Monographs on Crystallography 13; Oxford University Press: Oxford, U.K., 2002.

32 Kawano, M.; Haneda, T.; Hashizume, D.; Izumi, F.; Fujita, M. A selective instant synthesis of a coordination network and its ab initio powder structure determination. *Angew. Chem., Int. Ed.* **2008**, *47*, 1269–1271.

33 David, W. I. F.; Shankland, K.; van de Streek, J.; Pidcock, E.; Motherwell, W. D. S.; Cole, J. C. DASH: a program for crystal structure determination from powder diffraction data. *J. Appl. Crystallogr.* **2006**, *39*, 910–915.

34 Izumi, F.; Momma, K. Three-dimensional visualization in powder diffraction. *Solid State Phenom.* **2007**, *130*, 15–20.

35 Delgado-Friedrichs, O.; O'Keeffe, M.; Yaghi, O. M. Three-periodic nets and tilings: regular and quasiregular nets. *Acta Crystallogr., Sect. A* **2003**, *59*, 22–27.

36 Inokuma, Y.; Kawano, M.; Fujita, M. Crystalline molecular flasks. *Nat. Chem.* **2011**, *3*, 349–358.

37 Martí-Rujas, J.; Islam, N.; Hashizume, D.; Izumi, F.; Fujita, M.; Song, H. J.; Choi, H. C.; Kawano, M. Ab initio powder diffraction structure analysis of a host-guest network: short contacts between tetrathiafulvalene molecules in a pore. *Angew. Chem., Int. Ed.* **2011**, *50*, 6105–6108.

38 Kawano, M.; Fujita, M. Direct observation of crystalline-state guest exchange in coordination networks. *Coord. Chem. Rev.* **2007**, *251*, 2592–2605.

39 Toh, N. L.; Nagarathinam, M.; Vittal, J. J. Topochemical photodimerization in the coordination polymer $[\{(CF_3CO_2)(\mu O_2CCH_3)Zn\}_2(\mu\text{-bpe})_2]_n$ through single-crystal to single-crystal transformation. *Angew. Chem., Int. Ed.* **2005**, *44*, 2237–2241.

40 Biradha, K.; Fujita, M. A springlike 3D-coordination network that shrinks or swells in a crystal-to-crystal manner upon guest removal or readsorbtion. *Angew. Chem., Int. Ed.* **2002**, *41*, 3392–3395.

41 Ohara, K.; Martí-Rujas, J.; Haneda, T.; Kawano, M.; Hashizume, D.; Izumi, F.; Fujita, M. Formation of a thermally stable, porous coordination network via a crystalline-to-amorphous-to-crystalline phase transition. *J. Am. Chem. Soc.* **2009**, *131*, 3860–3861.

42 Martí-Rujas, J.; Islam, N.; Hashizume, D.; Izumi, F.; Fujita, M.; Kawano, M. Dramatic structural rearrangements in porous coordination networks. *J. Am. Chem. Soc.* **2011**, *133*, 5853–5860.

43 Martí-Rujas, J.; Matsushita, Y.; Izumi, F.; Fujita, M.; Kawano, M. Solid-liquid interface synthesis of microcrystalline porous coordination networks. *Chem. Commun.* **2010**, *46*, 6515–6517.

44 Schubert, U.; Hüsing, H. *Syntesis of Inorganic Materials*, 2nd ed.; Wiley-VCH: Weinheim, 2005.

45 Yang, C.; Kaipa, U.; Mather, Q. Z.; Wang, X.; Nesterov, V.; Venero, A. F.; Omary, M. A. Fluorous metal-organic frameworks with superior adsorption and hydrophobic properties toward oil spill cleanup and hydrocarbon storage. *J. Am. Chem. Soc.* **2011**, *133*, 18094–18097.

46 Vaidhyanathan, R.; Iremonger, S. S.; Shimizu, G. K. H.; Boyd, P. G.; Alavi, S.; Woo, T. K. Direct observation and quantification of CO_2 binding within an amine-functionalized nanoporous solid. *Science* **2010**, *330*, 650–653.

47 Metrangolo, P.; Neukirch, H.; Pilati, T.; Resnati, G. Halogen bonding based recognition processes: a world parallel to hydrogen bonding. *Acc. Chem. Res.* **2005**, *38*, 386–395.